JACC: CARDIOVASCULAR INTERVENTIONS
VOL. 7, NO. 12, 2014

ISSN 1936-8798/$36.00
PUBLISHED BY ELSEVIER INC.
http://dx.doi.org/10.1016/j.jcin.2014.06.025

Scaffold and Edge Vascular Response Following Implantation of Everolimus-Eluting Bioresorbable Vascular Scaffold

A 3-Year Serial Optical Coherence Tomography Study

Yao-Jun Zhang, MD, PhD,*† Javaid Iqbal, PhD,*‡ Shimpei Nakatani, MD,* Christos V. Bourantas, MD, PhD,* Carlos M. Campos, MD,* Yuki Ishibashi, MD, PhD,* Yun-Kyeong Cho, MD,* Susan Veldhof, RN,§ Jin Wang,§ Yoshinobu Onuma, MD, PhD,* Hector M. Garcia-Garcia, MD, PhD,* Dariusz Dudek, MD,‖ Robert-Jan van Geuns, MD, PhD,* Patrick W. Serruys, MD, PhD,*¶
on behalf of the ABSORB Cohort B Study Investigators

ABSTRACT

OBJECTIVES This study sought to investigate the in-scaffold vascular response (SVR) and edge vascular response (EVR) after implantation of an everolimus-eluting bioresorbable scaffold (BRS) using serial optical coherence tomography (OCT) imaging.

BACKGROUND Although studies using intravascular ultrasound have evaluated the EVR in metal stents and BRSs, there is a lack of OCT-based SVR and EVR assessment after BRS implantation.

METHODS In the ABSORB Cohort B (ABSORB Clinical Investigation, Cohort B) study, 23 patients (23 lesions) in Cohort B1 and 17 patients (18 lesions) in Cohort B2 underwent truly serial OCT examinations at 3 different time points (Cohort B1: post-procedure, 6 months, and 2 years; B2: post-procedure, 1 year, and 3 years) after implantation of an 18-mm scaffold. A frame-by-frame OCT analysis was performed at the 5-mm proximal, 5-mm distal edge, and 2-mm in-scaffold margins, whereas the middle 14-mm in-scaffold segment was analyzed at 1-mm intervals.

RESULTS The in-scaffold mean luminal area significantly decreased from baseline to 6 months or 1 year (7.22 ± 1.24 mm^2 vs. 6.05 ± 1.38 mm^2 and 7.64 ± 1.19 mm^2 vs. 5.72 ± 0.89 mm^2, respectively; both $p < 0.01$), but remained unchanged from then onward. In Cohort B1, a significant increase in mean luminal area of the distal edge was observed (5.42 ± 1.81 mm^2 vs. 5.58 ± 1.53 mm^2; $p < 0.01$), whereas the mean luminal area of the proximal edge remained unchanged at 6 months. In Cohort B2, the mean luminal areas of the proximal and distal edges were significantly smaller than post-procedure measurements at 3 years. The mean luminal area loss at both edges was significantly less than the mean luminal area loss of the in-scaffold segment at both 6-month and 2-year follow-up in Cohort B1 or at 1 year and 3 years in Cohort B2.

CONCLUSIONS This OCT-based serial EVR and SVR evaluation of the Absorb Bioresorbable Vascular Scaffold (Abbott Vascular, Santa Clara, California) showed less luminal loss at the edges than luminal loss within the scaffold. The luminal reduction of both edges is not a nosologic entity, but an EVR in continuity with the SVR, extending from the in-scaffold margin to both edges. (ABSORB Clinical Investigation, Cohort B [ABSORB B]; NCT00856856) (J Am Coll Cardiol Intv 2014;7:1361–9) © 2014 by the American College of Cardiology Foundation.

From the *Thoraxcenter, Erasmus Medical Center, Rotterdam, the Netherlands; †Nanjing First Hospital, Nanjing Medical University, Nanjing, China; ‡Department of Cardiovascular Science, University of Sheffield, Sheffield, United Kingdom; §Abbott Vascular, Diegem, Belgium; ‖Jagiellonian University, Krakow, Poland; and the ¶International Centre for Circulatory Health, NHLI, Imperial College London, London, United Kingdom. This study was sponsored by Abbott Vascular, Santa Clara, California. Dr. Geuns has received speaker honoraria from Abbott Vascular. S. Veldhof and J. Wang are full-time employees of Abbott Vascular. All other authors have reported that they have no relationships relevant to the contents of this paper to disclose.

Manuscript received February 3, 2014; revised manuscript received April 30, 2014, accepted June 19, 2014.

ABBREVIATIONS AND ACRONYMS

BMS = bare-metal stent(s)

BRS = bioresorbable scaffold(s)

BVS = bioresorbable vascular scaffold(s)

CI = confidence interval

DES = drug-eluting stent(s)

EVR = edge vascular response

IVUS = intravascular ultrasound

OCT = optical coherence tomography

SVR = in-scaffold vascular response

Restenosis in the segments adjacent to the proximal and distal edges of a permanent or transient coronary implant has been a concern for many years (1–5). In the metal drug-eluting stent (DES) era, studies demonstrated effective inhibition of neointimal hyperplasia reducing the risk of edge restenosis and the need for repeat intervention on the edges (6,7). Our group, using intravascular ultrasound (IVUS) imaging, previously investigated the edge vascular response (EVR) after implantation of fully bioresorbable scaffold (BRS) and reported a luminal area reduction at the proximal edge at 2-year follow-up (8).

SEE PAGE 1370

Optical coherence tomography (OCT) offers substantially superior resolution that allows a precise evaluation of luminal dimensions, edge dissections, and relevant vessel wall pathology (9–12). To date, no study has used serial OCT imaging to examine the EVR and its relationship with in-scaffold vascular response (SVR) at 3-year follow-up after BRS implantation. We hypothesized that the local changes in luminal dimensions at the edge of the Absorb Bioresorbable Vascular Scaffold (Absorb BVS) (Abbott Vascular, Santa Clara, California) are simply the extension of the changes in luminal dimension observed at the in-scaffold margins and not a separate pathological entity. This study aimed to evaluate the OCT-based SVR and EVR after Absorb BVS (Abbott Vascular) implantation in the ABSORB Cohort B (ABSORB Clinical Investigation, Cohort B) trial.

METHODS

STUDY DESIGN AND POPULATION. The ABSORB Cohort B trial was described in detail previously (12). Briefly, this was a nonrandomized, multicenter, single-arm trial that enrolled 101 patients (102 lesions) treated with the second-generation Absorb BVS (Abbott Vascular) (A complete list of the members of the ABSORB Cohort B Study appears in the Online Appendix). The participants were divided into 2 groups according to the pre-defined invasive follow-up: Cohort B1 at post-procedure, 6 months, and 2 years and Cohort B2 at post-procedure, 1 year, and 3 years. OCT was an optional examination conducted at selected centers with OCT capability and previous experience. The registry was approved by the ethics committee at each participating institution, and each patient gave written informed consent before inclusion.

STUDY DEVICE AND TREATMENT PROCEDURE. The Absorb BVS (Abbott Vascular) is a balloon-expandable scaffold consisting of a polymer backbone of poly-L-lactide coated with a thin layer of a 1:1

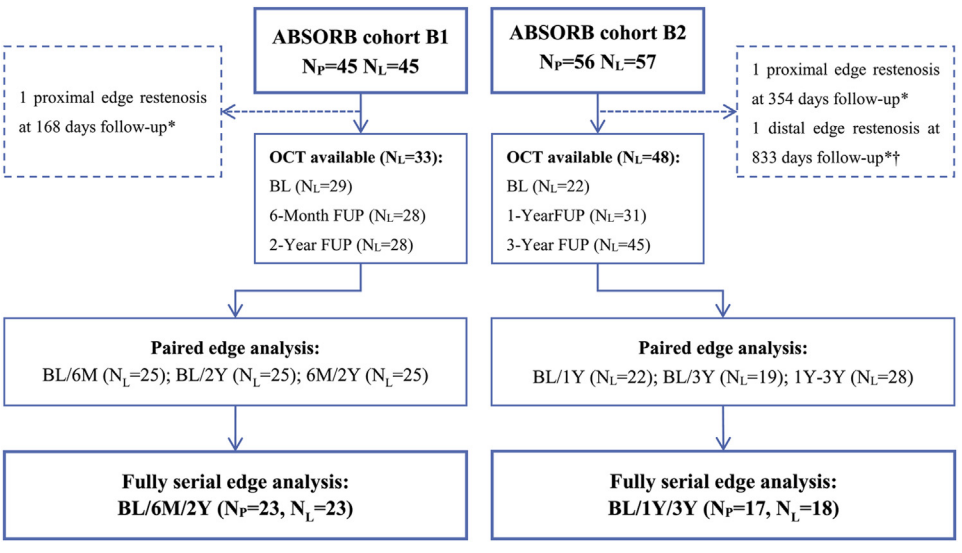

FIGURE 1 Flowchart of the Patients Included in the Current Analysis

*Edge restenoses in Cohort B that mandated repeat revascularization. †This case had in-segment restenosis at the distal margin of the scaffolded segment and distal edge. 1Y = 1 year; 2Y = 2 years; 3Y = 3 years; BL = baseline; FUP = follow-up; N_L = number of lesions; N_P = number of patients; OCT = optical coherent tomography.

mixture of amorphous poly-D,L-lactide polymer and the antiproliferative drug everolimus to form a drug-eluting coating matrix that contains 100 μg of everolimus per square centimeter of scaffold (13–15).

Target lesions were treated with routine interventional techniques, and pre-dilation was mandatory. The Absorb BVS (Abbott Vascular) inflation pressure did not exceed 16 atm, the burst pressure according to the product chart. Post-dilation with a balloon shorter than the implanted scaffold was at the discretion of the operator. OCT imaging was performed after optimal Absorb BVS (Abbott Vascular) implantation and at follow-up.

OCT ACQUISITIONS AND DATA ANALYSIS. OCT acquisitions were performed using 3 different commercially available systems: the M2 and M3 Time-Domain Systems and the C7XR Fourier-Domain System (LightLab Imaging, Westford, Massachusetts). OCT images were acquired at frame rates of 15.6, 20, and 100 frames/s with pullback speeds of 2, 3, and 20 mm/s in the M2 Time-Domain System (n = 11), M3 Time-Domain System (n = 11), and C7XR Fourier-Domain System (n = 101) (LightLab Imaging), respectively. All recordings were performed according to the recommended procedure for each OCT system (16). The OCT images acquired post-procedure and at follow-up were analyzed off-line, using proprietary LightLab Imaging software (St. Jude Medical Inc., St. Paul, Minnesota). Truly serial OCT data were defined as the patient undergoing OCT examinations at all 3 time points.

The SVR analysis included all 18-mm scaffold segments, analyzed at 1-mm intervals by an independent core laboratory (Cardialysis, Rotterdam, the Netherlands). The EVR analysis included the 5-mm proximal and distal edges, analyzed in a frame-by-frame fashion (128-μm interval for the M2, 150-μm interval for the M3, 200-μm interval for the C7). In addition, we performed a frame-by-frame analysis of changes in the lumen area at the 2-mm margins of the scaffold to explore the relationship between in-scaffold margins and the edges. The scaffold edge was defined as the first cross section exhibiting visible struts in a circumference <270° (10). If the 5-mm edge had a side branch with a vessel diameter ≥1.5 mm, the analysis included only frames between the scaffold's margin and the ostium of the side branch. If the vessel diameter of the side branch was <1.5 mm, only the frames at the ostium of the side branch were excluded. In addition, we excluded the cases that needed a bailout stent as well as the frames with insufficient assessment of the entire luminal circumference due to inadequate blood clearance or incomplete scanning perimeter. Edge dissection was defined as disruption of the endoluminal vessel surface at the proximal and distal edges (17).

TABLE 1 Baseline and Lesion Characteristics of Fully Serial OCT Available Patients

	Cohort B1 (n = 23)	Cohort B2 (n = 17)	Difference (95% CI)
Age, yrs	63.4 ± 9.8	61.6 ± 8.0	1.8 (−3.9 to 7.5)
Male	82.6	64.7	17.9 (−8.8 to 43.5)
Diabetes mellitus	4.3	5.9	−1.5% (−22.9 to 15.8)
Hypertension	52.2	70.6	−18.4 (−43.5 to 11.7)
Hypercholesterolemia	95.7	76.5	19.2 (−2.6 to 43.2)
Current smoker	21.7	29.4	−7.7% (−34.3 to 18.2)
Family history of CAD	52.2	66.7	−14.5% (−40.9 to 16.6)
Previous MI	43.5	12.5	31.0 (1.5–52.7)
History of PCI	26.1	11.8	14.3 (−12.0 to 36.4)
Unstable angina	17.4	5.9	11.5 (−12.0 to 31.8)
Target-lesion vessel, %			
LAD	26.1	11.1	15.0 (−10.6 to 36.9)
LCX	26.1	33.3	−7.3 (−33.9 to 19.3)
RCA	47.8	55.6	−7.7 (−35.0 to 21.4)
RVD before intervention	2.59 ± 0.40	2.57 ± 0.26	0.02 (−0.19 to 0.23)
Maximal balloon artery ratio	1.01 ± 0.15	1.05 ± 0.11	−0.04 (−0.12 to 0.05)
Maximal inflation pressure	18.4 ± 3.0	16.6 ± 5.3	1.8 (−1.1 to 4.7)

Values are mean ± SD or %.

CAD = coronary artery disease; CI = confidence interval; LAD = left anterior descending artery; LCX = left circumflex artery; MI = myocardial infarction; OCT = optical coherent tomography; PCI = percutaneous coronary intervention; RCA = right coronary artery; RVD = reference vessel diameter.

STATISTICAL ANALYSIS. Continuous variables are presented as mean ± SD or median (interquartile range). Binary variables are presented as count and percent. Absolute difference and 95% confidence interval (CI) of baseline characteristics was generated by normal approximation for continuous variables and Newcombe score method for binary variables. A paired *t* test or Wilcoxon signed rank test was used to compare SVR and EVR within groups at different time points. The normality of the data was determined with the D'Agostino Pearson test and verified by histogram plots. To evaluate the relationship of the lumen area

TABLE 2 In-Scaffold Vascular Response Analysis

	In-Scaffold Vascular Response (18 mm)			
Luminal Area Changes	Distal Subsegment (6 mm)	Middle Subsegment (6 mm)	Proximal Subsegment (6 mm)	p Value
Cohort B1				
6 months vs. baseline	−1.21 ± 0.79	−0.98 ± 0.68	−1.34 ± 0.79	0.27
2 yrs vs. 6 months	−0.44 ± 0.91	0.05 ± 1.46	0.12 ± 1.29	0.25
2 yrs vs. baseline	−1.65 ± 0.99	−0.94 ± 1.62	−1.22 ± 1.24	0.18
Cohort B2				
1 yr vs. baseline	−1.91 ± 1.24	−1.77 ± 1.10	−2.06 ± 0.87	0.73
3 yrs vs. 1 yr	−0.18 ± 0.93	0.26 ± 0.84	0.05 ± 0.72	0.29
3 yrs vs. baseline	−2.10 ± 1.59	−1.51 ± 1.23	−2.00 ± 1.03	0.36

Values are mean ± SD.

TABLE 3 Edge Vascular Response Analysis

Luminal Area	Cohort B1		Cohort B2	
Distal edge, 5 mm	6M	2Y	1Y	3Y
Baseline	5.42 ± 1.81		5.78 ± 2.04	
FUP (6M/2Y, 1Y/3Y)	5.58 ± 1.53	5.26 ± 1.40	5.63 ± 1.45	5.29 ± 1.77
Difference	0.19 ± 1.05	−0.16 ± 1.24	−0.14 ± 1.25	−0.49 ± 1.17
p value (BL vs. FUP)	<0.01	0.03	0.11	<0.01
Proximal edge, 5 mm	6M	2Y	1Y	3Y
Baseline	6.84 ± 2.86		7.27 ± 2.01	
FUP (6M/2Y, 1Y/3Y)	6.76 ± 2.63	6.75 ± 2.60	6.66 ± 1.74	6.51 ± 1.63
Difference	−0.07 ± 1.14	−0.08 ± 1.13	−0.61 ± 1.33	−0.76 ± 1.57
p value (BL vs. FUP)	0.31	0.25	<0.01	<0.01

Values are mean ± SD.
6M = 6 months; 1Y = 1 year; 2Y = 2 years; 3Y = 3 years; BL = baseline; FUP = follow-up.

within different segments of the scaffold (3 subsegments: proximal, middle, and distal), multilevel generalized estimating equation model fitting, with the mean lumen area as the response and the subsegments and the follow-up visits as categorical variables, were nested within each patient. Multiple comparisons were conducted without adjustment. Statistical significance was assumed at $p < 0.05$. All statistical analyses were performed with SAS version 9.1.3 (SAS Institute Inc., Cary, North Carolina).

RESULTS

STUDY POPULATION AND OCT ACQUISITION. A flowchart of the subjects included in the current

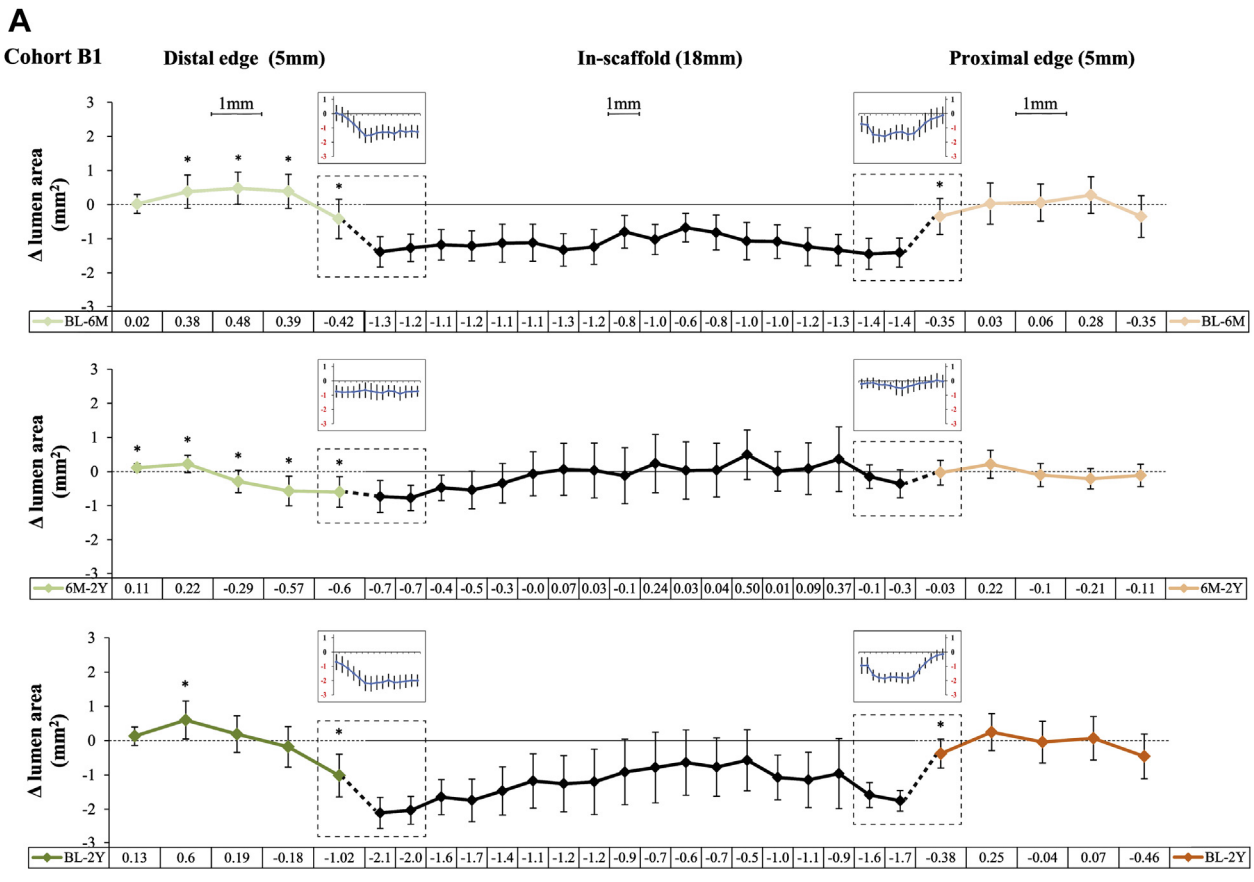

FIGURE 2 Scaffold and Its EVR

The images present the global mean luminal area changes including in-scaffold, 5-mm proximal and distal edges at follow-up. **(A)** Cohort B1. **(B)** Cohort B2. Mean luminal area of the 18-mm in-scaffold segment significantly decreased from baseline to 6-month or 1-year follow-up, but no change from 6 months to 2 years or 1 year to 3 years. The EVR analysis showed an increase in mean luminal area at the distal edge at 6 months and a reduction at both the proximal and distal edges at long-term follow-up. The transitional regions with a 200-μm interval analysis are presented in the embedded panels, indicating a continuous pattern of luminal reduction extending from the in-scaffold margins to the first 1 mm of proximal and distal edges. *Indicates a significant change in mean luminal area in each 1-mm interval at the proximal or distal edge ($p < 0.05$). EVR = edge vascular response; other abbreviations as in Figure 1.

analysis is shown in Figure 1. A total of 183 OCT pullbacks at baseline and follow-up were performed in 80 patients (81 lesions). Twenty-three patients (23 lesions) in Cohort B1 and 17 patients (18 lesions) in Cohort B2 had truly serial OCT examinations at 3 different time points. Three patients who had a target lesion revascularization did not undergo OCT examination before the reintervention.

Baseline characteristics of the patients with truly serial OCT pullbacks are shown in Table 1. There was a greater prevalence of patients with previous myocardial infarction (43.5% vs. 12.5%; difference: 31.0%; 95% CI: 1.5% to 52.7%) and lesions in the left anterior descending artery in Cohort B1 (26.1% vs. 11.1%; difference: 15.0%; 95% CI: −10.6% to 36.9%) than in Cohort B2.

SVR ANALYSIS. In Cohort B1, there was a significant reduction in mean in-scaffold luminal area at 6 months (7.22 ± 1.24 mm^2 vs. 6.05 ± 1.38 mm^2, $p < 0.01$). However, the mean luminal area remained unchanged from 6 months to 2 years (5.97 ± 1.61 mm^2, $p = 0.75$). Similarly, in Cohort B2, there was a significant reduction in mean in-scaffold luminal area from baseline to 1 year (7.64 ± 1.19 mm^2 vs. 5.72 ± 0.89 mm^2, $p < 0.01$), but no change from 1 year to 3 years (5.81 ± 1.29 mm^2, $p = 0.60$).

At 3-year follow-up, there was no significant difference in behavior of the 3 in-scaffold subsegments (proximal, middle, and distal) (Table 2). The mean luminal area of proximal and middle subsegments numerically increased from 6 months to 2 years or 1 year to 3 years (B1: 0.12 ± 1.29 mm^2, 0.05 ± 1.46 mm^2; B2: 0.05 ± 0.72 mm^2, 0.26 ± 0.84 mm^2; respectively), whereas the mean luminal area of the distal segment numerically decreased (B1: −0.44 ± 0.91 mm^2, −0.18 ± 0.93 mm^2).

EVR ANALYSIS. The changes in mean luminal area of the proximal and distal edges at different time points are shown in Table 3. In Cohort B1, a significant increase in mean luminal area at the distal edge (5-mm

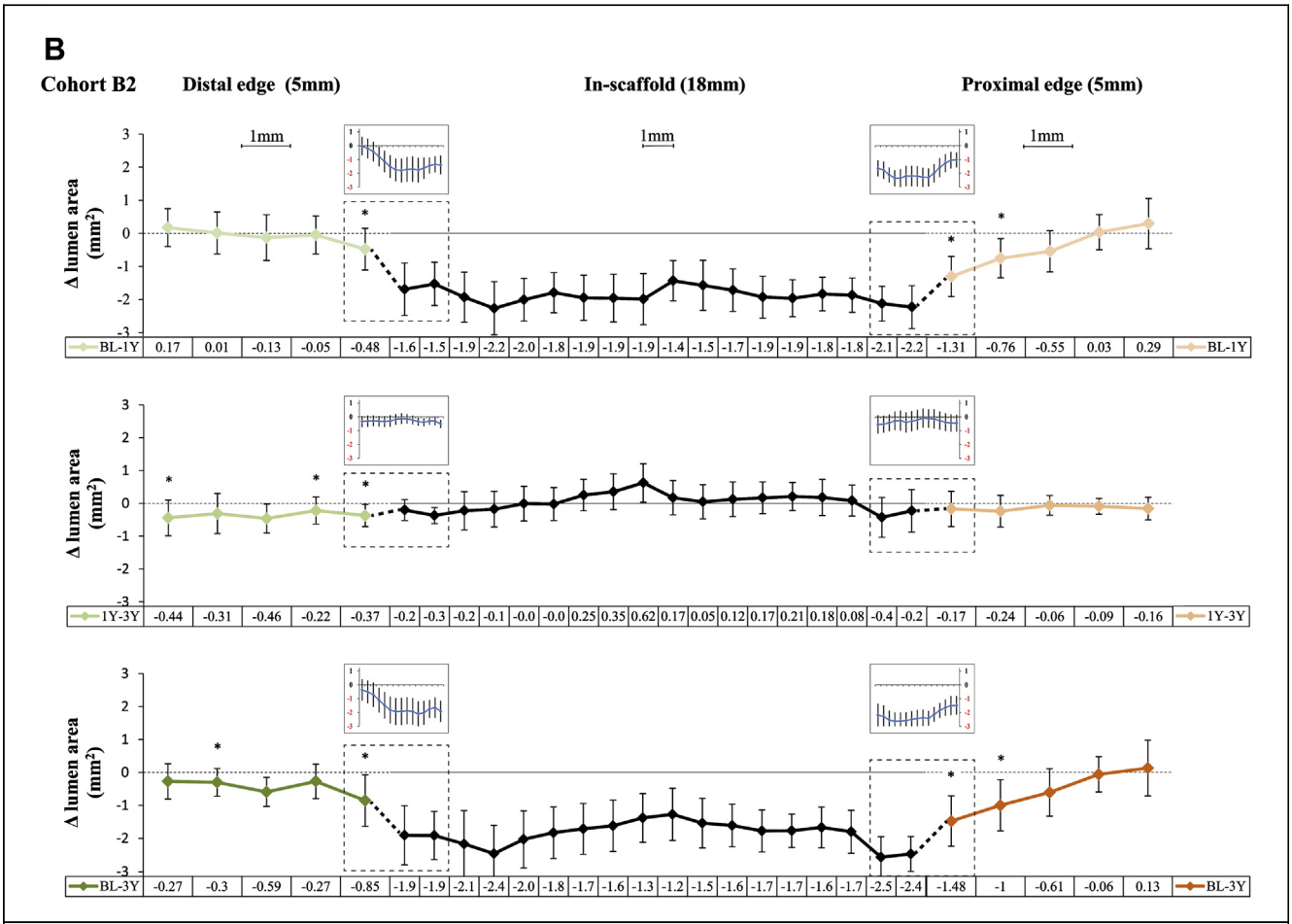

FIGURE 2 Continued

TABLE 4 Overall Vascular Response Analysis

Luminal Area Changes	Distal Edge, 5 mm	In-Scaffold, 18 mm	Proximal Edge, 5 mm	p Value (Distal vs. In-Scaffold)	p Value (Proximal vs. In-Scaffold)
Cohort B1					
6 months vs. baseline, mm^2	0.16 ± 1.05	−1.18 ± 1.06	−0.07 ± 1.14	<0.01	<0.01
2 years vs. baseline, mm^2	−0.16 ± 1.24	−1.23 ± 1.64	−0.08 ± 1.13	<0.01	<0.01
Cohort B2					
1 year vs. baseline, mm^2	−0.14 ± 1.25	−1.88 ± 1.29	−0.61 ± 1.33	<0.01	<0.01
3 years vs. baseline, mm^2	−0.49 ± 1.17	−1.85 ± 1.50	−0.76 ± 1.56	<0.01	<0.01

Values are mean ± SD.

segment) was observed at 6 months (5.42 ± 1.81 mm^2 vs. 5.58 ± 1.53 mm^2, $p < 0.01$) (Figure 2A), whereas at the proximal edge (5-mm segment), the mean luminal area remained unchanged (6.84 ± 2.86 mm^2 vs. 6.76 ± 2.63 mm^2, $p = 0.31$). In Cohort B2, the mean luminal area at the distal edge was unchanged at 1-year follow-up (5.78 ± 1.45 mm^2 vs. 5.63 ± 1.45 mm^2, $p = 0.11$) (Figure 2B). At 3-year follow-up, a significant reduction in the mean luminal area was observed at both edges (distal: 5.78 ± 2.04 mm^2 vs. 5.29 ± 1.77 mm^2; proximal: 7.27 ± 2.01 mm^2 vs. 6.51 ± 1.63 mm^2; both $p < 0.01$).

PATTERN OF CHANGES IN LUMINAL DIMENSIONS FROM IN-SCAFFOLD MARGINS TO EDGES. At all time points, reduction in the luminal area was observed in the first 1 mm of the edges, both proximally and distally, indicating a continuous pattern of luminal reduction extending from the scaffold margin to the proximal or distal edge (Figure 2). The overall reduction in mean luminal area at both edges was significantly less than the in-scaffold segments (all $p < 0.05$) (Table 4).

EDGE RESTENOSIS, EDGE DISSECTION, AND STENT THROMBOSIS. Of 101 patients in the entire ABSORB Cohort B trial, 2 patients (2.0%) had proximal edge restenosis and 1 patient (1%) had distal edge restenosis. Patients with the proximal edge restenosis had a repeat revascularization at day 168 and day 383, respectively. The patient with the distal edge restenosis had a repeat revascularization at day 833. These 3 patients were treated without previous OCT to examine edge restenosis. In 2 of these patients, a geographic miss (injured or diseased segment not covered by the device, balloon-artery ratio <0.9 or >1.3) was previously reported (15).

In total, 12 proximal (24%) and 21 distal (42%) edge dissection flaps were observed post-procedure. In the truly serial OCT analysis, 9 proximal (21%) and 16 distal (38%) edge dissection flaps were identified post-procedure, which decreased to 1 proximal (2%) and 2 distal (5%) at 6 months, only proximal 1 (2%) at 1-year follow-up, and none at 2- and 3-year follow-up (Figure 3). No scaffold thrombosis was reported in this trial.

DISCUSSION

This study, for the first time, reported OCT-derived EVR and SVR evaluation after Absorb BVS (Abbott Vascular) implantation at mid- and long-term follow-up. The primary findings are the following: 1) an increase in mean luminal area at the distal edge at 6 months; 2) a reduction in the mean luminal area at both edges at long-term (2- or 3-year) follow-up; 3) reduction in luminal area at the in-scaffold segment from baseline to 6 or 12 months, but no change from then onward. A uniform pattern of luminal reduction extending from the in-scaffold margins to the first 1-mm of the proximal and distal edges of the scaffold is also demonstrated, suggesting that the edge changes in luminal dimension is not a nosologic entity, but a progressive transition in luminal dimension from the in-scaffold margin to the edges.

EVOLUTION OF DEVICES AND EVR. The introduction of coronary metal stents has markedly reduced the risk of restenosis (14). The EVR in the era of bare metal stents (BMS) was mainly due to an increase in plaque and medial area and reduction in luminal area within the first 1 to 2 mm of the device (15,18). Radioactive stents, developed to reduce restenosis, were proved to be safe in initial studies (19,20), but led to a profound edge effect defined angiographically as a diameter stenosis of >50% at the proximal and distal stent edges (2,3). In the DES era, the EVR can also be influenced by the drug and polymer incorporated into the stent (21). A high degree of variability in EVR was identified among the different DES types (5). In the TAXUS II trial, paired-edge analyses with IVUS showed a significant increase in luminal area at the distal edge of paclitaxel-eluting stent compared with the BMS at 6 months, whereas a significant decrease in the luminal area was observed at the proximal edge (22). The beneficial effect of the paclitaxel-eluting stent was most notable in the area closest to its distal edge (23). Trials with the Endeavor stent (Medtronic, Minneapolis, Minnesota) demonstrated a reduction in the luminal area at both the proximal and distal edges, mainly due to negative remodeling, plaque growth, and rapid elution of zotarolimus (24,25). However, serial IVUS

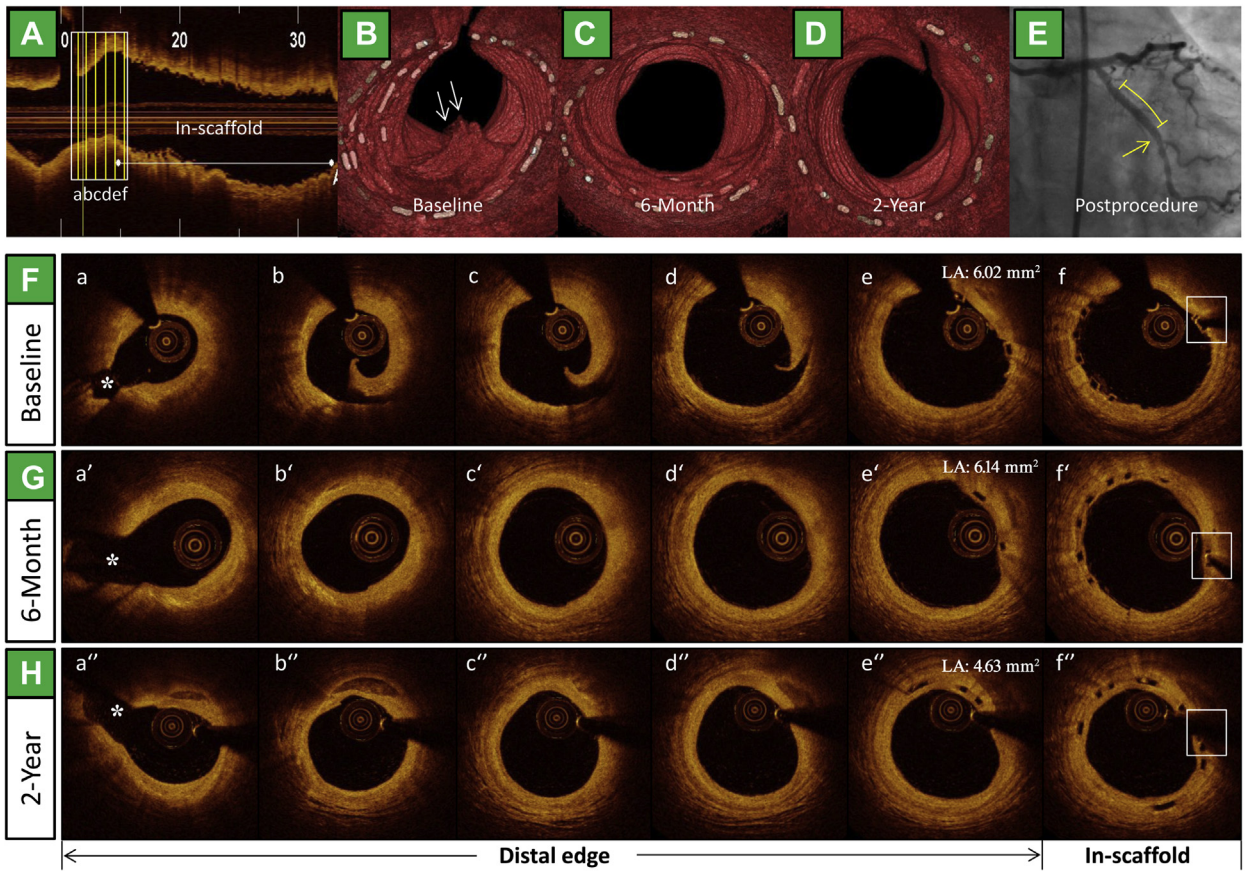

FIGURE 3 Dissections at the Distal Edge

(A) Longitudinal view of patients with distal dissection. **(B)** Three-dimensional reconstruction of optical coherence tomography pullbacks show that dissection is visible at distal edge **(double white arrow)**. **(C, D)** Three-dimensional reconstruction at 6-month and 2-year follow-up showed that dissection has healed. **(E)** No distal edge dissection **(arrow)** is visible from the post-procedure angiograms. The **curved line** indicates the scaffolded segment. **(F)** Dissection extends into at least the media from multiple cross-sectional views. **(G)** Increased luminal area without visible dissection at 6-month follow-up. **(H)** The luminal area decreased with detected calcific tissue at 2-year follow-up. LA = lumen area. *Indicates a side branch.

examination in sirolimus- and everolimus-eluting stents revealed an enlargement of the luminal area at the distal edge (26-28). Our results are in agreement with those of previous reports on metal everolimus-eluting stents (28), with a significant increase in the distal-edge luminal area and a nonsignificant decrease in the proximal edge at 6-month follow-up. The difference in behavior of the 2 edges can partially be explained by downstream diffusion of antiproliferative drug to the distal edge (21).

IN-DEPTH ANALYSIS OF EVR AND SVR. IVUS imaging has contributed to our understanding of EVR after BRS implantation. However, this approach has inherent limitations (e.g., poor resolution, cardiac motion artifacts) and makes it difficult to assess EVR precisely (29-31). The present study, performed with OCT, for the first time evaluated EVR in frame-by-frame (≤200 μm) fashion after Absorb BVS (Abbott Vascular) implantation and provided additional insights into the changes in luminal dimensions at the proximal and distal edges.

Our previous IVUS-based study demonstrated a nonsignificant reduction in luminal area at the distal edge at 6 months (32); however, accurate assessment with OCT has documented it to be a significant change. By the virtue of the high resolution of OCT, we also demonstrated that the pattern of in-scaffold luminal reduction extended progressively from the in-scaffold margins to the contiguous first 1 mm of the edges outside the scaffold, both proximally and distally, presumably related to neointimal

hyperplasia or neoatherosclerosis (33). In addition, the discrepancy with previous IVUS observations can also be attributed to the nonserial nature of the data in previous IVUS studies. Thus, we believe that OCT-based EVR evaluation with truly serial data can provide more reliable and precise information.

Finally, the SVR analysis presented here is consistent with the previous final 3-year report of the ABSORB Cohort B study (32). The analysis of changes in mean luminal area of different in-scaffold subsegments using a generalized estimating equation model did not show any significant difference in vascular response; however, there was a numerical increase in luminal area in the middle subsegment from 1 year to 3 years. Preclinical studies of the BRS have demonstrated that late luminal positive remodeling was observed at late follow-up (34). It will be interesting to re-evaluate this subsegment behavior at 5-year follow-up of the ABSORB Cohort B study.

CLINICAL IMPLICATIONS. The Absorb BVS (Abbott Vascular) does not produce a pathological edge effect that was seen with BMS or notoriously with radioactive stents. The stable luminal area after 6 to 12 months without late catch-up is a potential superiority of BRS over metal DES. In the ABSORB Cohort B trial, there were only 3 cases of edge restenosis, and 2 of them could be attributed to longitudinal geographic miss (13). Edge dissections, considered to be a trigger for early stent thrombosis, were often detected by post-procedure OCT in the present study; however, most of these dissections healed within 6 months, without any clinical adverse events.

STUDY LIMITATIONS. First, the number of patients in the current study is small; however, it is the largest and longest series available to date, and due to the truly serial OCT data, potential patient-to-patient variability was minimized. Second, OCT examination was not available for patients undergoing repeat revascularization, and, therefore, we decided to exclude these patients from this analysis. Finally, OCT cannot visualize external elastic lamina due to its low penetration, and, hence, changes in plaque media or vessel area cannot be assessed adequately.

CONCLUSIONS

In this study, truly serial OCT imaging was used to assess the EVR and SVR after Absorb BVS (Abbott Vascular) implantation up to 3-year follow-up. We found a significant increase in the luminal area at the distal edge at 6-month follow-up. However, at longer term (1, 2, and 3 years), the luminal area decreased at both edges, resulting in a repeat revascularization rate of 3%. In-scaffold luminal area significantly decreased from post-procedure to 6 months or 1 year, but remained unchanged from then onward. A continuous pattern of luminal loss extending from the in-scaffold margins to the first 1-mm of scaffold edges has suggested that the changes in luminal area at the edge of a BRS is not a nosologic entity in itself, but an extension of the in-scaffold response to the edges.

REPRINT REQUESTS AND CORRESPONDENCE: Dr. Patrick W. Serruys, International Centre for Circulatory Health, NHLI, Imperial College London, Royal Brompton Campus, London SW7 2AZ, United Kingdom. E-mail: p.w.j.c.serruys@gmail.com.

REFERENCES

1. Albiero R, Nishida T, Adamian M, et al. Edge restenosis after implantation of high activity (32)P radioactive beta-emitting stents. Circulation 2000;101:2454–7.

2. van Der Giessen WJ, Regar E, Harteveld MS, et al. "Edge Effect" of (32)p radioactive stents is caused by the combination of chronic stent injury and radioactive dose falloff. Circulation 2001;104:2236–41.

3. Serruys PW, Kay IP. I like the candy, I hate the wrapper: the (32)P radioactive stent. Circulation 2000;101:3–7.

4. Serruys PW, Ormiston JA, Sianos G, et al. Actinomycin-eluting stent for coronary revascularization: a randomized feasibility and safety study: the ACTION trial. J Am Coll Cardiol 2004;44:1363–7.

5. Gogas BD, Garcia-Garcia HM, Onuma Y, et al. Edge vascular response after percutaneous coronary intervention: an intracoronary ultrasound and optical coherence tomography appraisal: from radioactive platforms to first- and second-generation drug-eluting stents and bioresorbable scaffolds. J Am Coll Cardiol Intv 2013;6:211–21.

6. Serruys PW, Silber S, Garg S, et al. Comparison of zotarolimus-eluting and everolimus-eluting coronary stents. N Engl J Med 2010;363:136–46.

7. Windecker S, Serruys PW, Wandel S, et al. Biolimus-eluting stent with biodegradable polymer versus sirolimus-eluting stent with durable polymer for coronary revascularisation (LEADERS): a randomised non-inferiority trial. Lancet 2008;372:1163–73.

8. Gogas BD, Bourantas CV, Garcia-Garcia HM, et al. The edge vascular response following implantation of the Absorb everolimus-eluting bioresorbable vascular scaffold and the XIENCE V metallic everolimus-eluting stent. First serial follow-up assessment at six months and two years: insights from the first-in-man ABSORB Cohort B and SPIRIT II trials. EuroIntervention 2013;9:709–20.

9. Ormiston JA, Serruys PW, Onuma Y, et al. First serial assessment at 6 months and 2 years of the second generation of absorb everolimus-eluting bioresorbable vascular scaffold: a multi-imaging modality study. Circ Cardiovasc Interv 2012;5:620–32.

10. Gogas BD, Onuma Y, van Geuns RJ, Serruys PW. The edge vascular response following implantation of a fully bioresorbable device: 'a miss always counts'. Int J Cardiol 2012;158:455–7.

11. Gogas BD, Muramatsu T, Garcia-Garcia HM, et al. In vivo three dimensional optical coherence tomography. A novel imaging modality to visualize the edge vascular response. Int J Cardiol 2013;164:e35–7.

12. Serruys PW, Onuma Y, Dudek D, et al. Evaluation of the second generation of a bioresorbable everolimus-eluting vascular scaffold for the treatment of de novo coronary artery stenosis: 12-month clinical and imaging outcomes. J Am Coll Cardiol 2011;58:1578–88.

13. Nakatani S, Onuma Y, Ishibashi Y, et al. Early (before 6 months), late (6-12 months) and very late (after 12 months) angiographic scaffold restenosis in the ABSORB Cohort B trial. EuroIntervention 2014 Feb 27 [E-pub ahead of print].

14. Iqbal J, Gunn J, Serruys PW. Coronary stents: historical development, current status and future directions. Br Med Bull 2013;106:193–211.

15. Weissman NJ, Wilensky RL, Tanguay JF, et al. Extent and distribution of in-stent intimal hyperplasia and edge effect in a non-radiation stent population. Am J Cardiol 2001;88:248–52.

16. Tearney GJ, Regar E, Akasaka T, et al. Consensus standards for acquisition, measurement, and reporting of intravascular optical coherence tomography studies: a report from the International Working Group for Intravascular Optical Coherence Tomography Standardization and Validation. J Am Coll Cardiol 2012;59:1058–72.

17. Muramatsu T, Garcia-Garcia HM, Onuma Y, et al. Intimal flaps detected by optical frequency domain imaging in the proximal segments of native coronary arteries. Circ J 2013;77:2327–33.

18. Popma JJ, Leon MB, Moses JW, et al. Quantitative assessment of angiographic restenosis after sirolimus-eluting stent implantation in native coronary arteries. Circulation 2004;110:3773–80.

19. King SB 3rd, Williams DO, Chougule P, et al. Endovascular beta-radiation to reduce restenosis after coronary balloon angioplasty: results of the beta energy restenosis trial (BERT). Circulation 1998;97:2025–30.

20. Condado JA, Waksman R, Gurdiel O, et al. Long-term angiographic and clinical outcome after percutaneous transluminal coronary angioplasty and intracoronary radiation therapy in humans. Circulation 1997;96:727–32.

21. Wakabayashi K, Waksman R, Weissman NJ. Edge effect from drug-eluting stents as assessed with serial intravascular ultrasound: a systematic review. Circ Cardiovasc Interv 2012;5:305–11.

22. Serruys PW, Degertekin M, Tanabe K, et al. Vascular responses at proximal and distal edges of paclitaxel-eluting stents: serial intravascular ultrasound analysis from the TAXUS II trial. Circulation 2004;109:627–33.

23. Weissman NJ, Ellis SG, Grube E, et al. Effect of the polymer-based, paclitaxel-eluting TAXUS Express stent on vascular tissue responses: a volumetric intravascular ultrasound integrated analysis from the TAXUS IV, V, and VI trials. Eur Heart J 2007;28:1574–82.

24. Sakurai R, Hongo Y, Yamasaki M, et al. Detailed intravascular ultrasound analysis of Zotarolimus-eluting phosphorylcholine-coated cobalt-chromium alloy stent in de novo coronary lesions (results from the ENDEAVOR II trial). Am J Cardiol 2007;100:818–23.

25. Waseda K, Miyazawa A, Ako J, et al. Intravascular ultrasound results from the ENDEAVOR IV trial: randomized comparison between zotarolimus- and paclitaxel-eluting stents in patients with coronary artery disease. J Am Coll Cardiol Intv 2009;2:779–84.

26. Jimenez-Quevedo P, Sabate M, Angiolillo DJ, et al. Vascular effects of sirolimus-eluting versus bare-metal stents in diabetic patients: three-dimensional ultrasound results of the Diabetes and Sirolimus-Eluting Stent (DIABETES) Trial. J Am Coll Cardiol 2006;47:2172–9.

27. Jensen LO, Maeng M, Mintz GS, et al. Serial intravascular ultrasound analysis of peri-stent remodeling and proximal and distal edge effects after sirolimus-eluting or paclitaxel-eluting stent implantation in patients with diabetes mellitus. Am J Cardiol 2009;103:1083–8.

28. Shimohama T, Ako J, Yamasaki M, et al. SPIRIT III JAPAN versus SPIRIT III USA: a comparative intravascular ultrasound analysis of the everolimus-eluting stent. Am J Cardiol 2010;106:13–7.

29. Arbab-Zadeh A, DeMaria AN, Penny WF, Russo RJ, Kimura BJ, Bhargava V. Axial movement of the intravascular ultrasound probe during the cardiac cycle: implications for three-dimensional reconstruction and measurements of coronary dimensions. Am Heart J 1999;138:865–72.

30. von BC, de Vrey EA, Mintz GS, et al. ECG-gated three-dimensional intravascular ultrasound: feasibility and reproducibility of the automated analysis of coronary lumen and atherosclerotic plaque dimensions in humans. Circulation 1997;96:2944–52.

31. Bruining N, von BC, de Feyter PJ, et al. ECG-gated versus nongated three-dimensional intracoronary ultrasound analysis: implications for volumetric measurements. Cathet Cardiovasc Diagn 1998;43:254–60.

32. Gogas BD, Serruys PW, Diletti R, et al. Vascular response of the segments adjacent to the proximal and distal edges of the ABSORB everolimus-eluting bioresorbable vascular scaffold: 6-month and 1-year follow-up assessment: a virtual histology intravascular ultrasound study from the first-in-man ABSORB cohort B trial. J Am Coll Cardiol Intv 2012;5:656–65.

33. Serruys PW, Onuma Y, Garcia-Garcia HM, et al. Dynamics of vessel wall changes following the implantation of the Absorb everolimus-eluting bioresorbable vascular scaffold: a multi-imaging modality study at 6, 12, 24 and 36 months. EuroIntervention 2014;9:1271–84.

34. Strandberg E, Zeltinger J, Schulz DG, Kaluza GL. Late positive remodeling and late lumen gain contribute to vascular restoration by a non-drug eluting bioresorbable scaffold: a four-year intravascular ultrasound study in normal porcine coronary arteries. Circ Cardiovasc Interv 2012;5:39–46.

KEY WORDS Absorb BVS, bioresorbable scaffold, edge vascular response, in-scaffold vascular response, optical coherence tomography

APPENDIX For a complete list of the ABSORB Cohort B study investigators, please see the online version of this article.